AGU PUBLICATIONS

Geophysical Research Letters

RESEARCH LETTER
10.1002/2016GL068865

Key Points:
- Inertial Alfvén waves have an electric field aligned with the mean magnetic field that is predicted to modify electron motion
- Laboratory measurements of electron sloshing at the Alfvén wave frequency verify predictions
- The magnetic field-aligned electric field of inertial Alfvén waves is also expected to resonantly accelerate auroral electrons

Correspondence to:
J. W. R. Schroeder,
james-schroeder@uiowa.edu

Citation:
Schroeder, J. W. R., F. Skiff, C. A. Kletzing, G. G. Howes, T. A. Carter, and S. Dorfman (2016), Direct measurement of electron sloshing of an inertial Alfvén wave, *Geophys. Res. Lett.*, *43*, 4701–4707, doi:10.1002/2016GL068865.

Received 31 MAR 2016
Accepted 21 APR 2016
Accepted article online 28 APR 2016
Published online 18 MAY 2016

Direct measurement of electron sloshing of an inertial Alfvén wave

J. W. R. Schroeder[1], F. Skiff[1], C. A. Kletzing[1], G. G. Howes[1], T. A. Carter[2], and S. Dorfman[2]

[1]Department of Physics and Astronomy, University of Iowa, Iowa City, Iowa, USA, [2]Department of Physics and Astronomy, University of California, Los Angeles, California, USA

Abstract We report laboratory measurements of the parallel current carried by suprathermal electrons associated with inertial Alfvén wave excitation in the laboratory. The experiments presented here use a novel wave absorption diagnostic that measures the suprathermal tails of the electron distribution parallel to the mean magnetic field. The diagnostic is used to probe the electron distribution as an inertial Alfvén wave propagates along the mean magnetic field. These results identify, for the first time, the periodic motion of suprathermal electrons participating in the inertial Alfvén wave itself, in agreement with predictions from linear kinetic theory.

1. Introduction

Alfvén waves and their interaction with fast electrons are implicated in a large number of physical phenomena in space and astrophysical plasmas. For example, the interaction of Alfvén waves with energetic particles impacts heating of the solar corona [*Hollweg*, 1974; *McIntosh et al.*, 2011] and cosmic ray transport [*Skilling*, 1975; *Bell*, 1978]. Alfvén waves propagating from the magnetotail along magnetic field lines toward the ionosphere are believed to accelerate electrons sufficiently to generate discrete auroral arcs [*Hasegawa*, 1976; *Goertz and Boswell*, 1979; *Lysak*, 1985; *Kletzing*, 1994; *Stasiewicz et al.*, 2000; *Kletzing and Hu*, 2001; *Keiling*, 2009]. While rockets and satellites routinely measure particle velocity distributions, the point of measurement is moving in time and space, and wave structures are simultaneously evolving as they propagate past the measurement platform. Consequently, in situ results have been mostly limited to statistical statements about the connection of Alfvén waves and electron acceleration. In one such statistical survey, the FAST satellite recorded a 31% conjunction of Alfvén waves and downward electron fluxes onto the ionosphere [*Chaston et al.*, 2007]. While laboratory plasmas avoid the space-time ambiguity of rocket and satellite measurements, laboratory investigations have not been successful in demonstrating this connection because wave-particle interactions with electrons in the tail of the distribution function are difficult to observe with traditional methods. The laboratory experiments presented here achieve a new level of sensitivity to the electron population in the tail of the distribution function using a novel wave absorption diagnostic.

This letter presents what we believe to be the first direct measurement of parallel electron motion associated with a propagating Alfvén wave. In section 2, we present the experimental setup for generating and measuring Alfvén waves as well as the wave absorption diagnostic for measuring the reduced parallel distribution function $g_e(v_z)$. Section 3 describes the linear kinetic theory used to model the experiment. Experimental and theoretical results are compared in section 4, and the conclusions and future experiments are discussed in section 5.

2. Experiment

This experiment was designed to observe modifications of the reduced parallel electron distribution function, $g_e(v_z)$, associated with an Alfvén wave in laboratory conditions relevant to the auroral magnetosphere (2–4 R_E in geocentric coordinates). The three primary components of this experiment are the antenna that launches Alfvén waves, the probes used to quantify the Alfvén wave, and the diagnostic that measures the reduced parallel electron distribution function $g_e(v_z)$, which is defined as

$$g_e(v_z) = \int_{-\infty}^{\infty}\int_{-\infty}^{\infty} f_e(v_z, v_x, v_y)\mathrm{d}v_x\mathrm{d}v_y, \tag{1}$$

where the equilibrium magnetic field is $\mathbf{B}_0 = B_0\hat{\mathbf{z}}$.

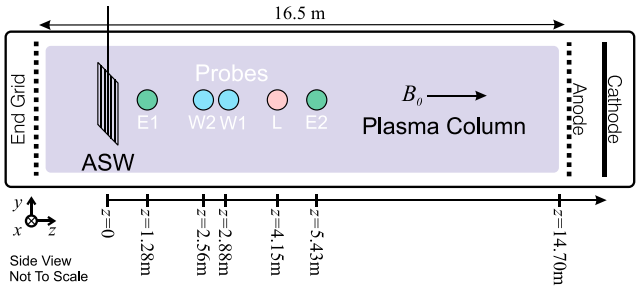

Figure 1. Experimental setup in the LaPD. Elsasser probes E1 and E2 observe the perpendicular wavefields $\mathbf{B}_\perp$ and $\mathbf{E}_\perp$ in the *x*-*y* plane. Whistler probes W1 and W2 are used to measure the parallel electron distribution function $g_e(v_z)$. A scanning Langmuir probe, denoted as *L* above, measures electron density and temperature.

The experiments were performed in the Large Plasma Device (LaPD) [*Gekelman et al.*, 2016], an NSF/DOE user facility at the University of California, Los Angeles. The experiment used a 10 ms discharge of hydrogen plasma, and the discharge was repeated at 1 Hz. The plasma is very repeatable from discharge to discharge, and the slight variations of measured quantities between discharges are random and can be reduced by ensemble averaging. Figure 1 shows a schematic of the locations of various probes used to make measurements. The swept Langmuir probe was used to find the electron density $n_e = 1.0 \times 10^{12}$ cm^{-3} and electron temperature $T_e = 2.2$ eV. Langmuir probe measurements of n_e were calibrated to a nearby line-integrated measurement from a microwave interferometer. The externally applied background magnetic field is $B_0 = 1.8$ kG. Based on these plasma conditions, the electron skin depth is $\delta_e = 0.53$ cm and $v_{te}/v_A = 0.16$ where $v_{te} = (kT_e/m_e)^{1/2}$ is the electron thermal speed and v_A is the Alfvén speed. These parameters are relevant to the inertial Alfvén wave where $v_{te}/v_A < 1$ and are appropriate for the auroral magnetosphere. During the discharge sequence, the Alfvén wave is excited for 1 ms at $t = 4$ ms after the start of the discharge, and all data are collected as the Alfvén wave passes the probes.

Alfvén waves are excited using the *Arbitrary Spatial Waveform* (ASW) antenna [*Thuecks et al.*, 2009], depicted in Figure 2a. The antenna consists of a series of conducting grid pieces that draw currents directly from the plasma. The currents collected by the ASW antenna flow parallel to the fixed, externally applied, magnetic field $\mathbf{B}_0$. By oscillating the current collected by the antenna, an oscillating magnetic field perturbation is produced, thereby launching an Alfvén wave. The amplitude of the current collected by each grid piece can be individually controlled, allowing a pattern to be established in $\hat{\mathbf{x}}$ that defines $\mathbf{k}_\perp$. The Alfvén wave amplitude produced by the ASW antenna is limited by the magnitude of the current that can be drawn from the plasma.

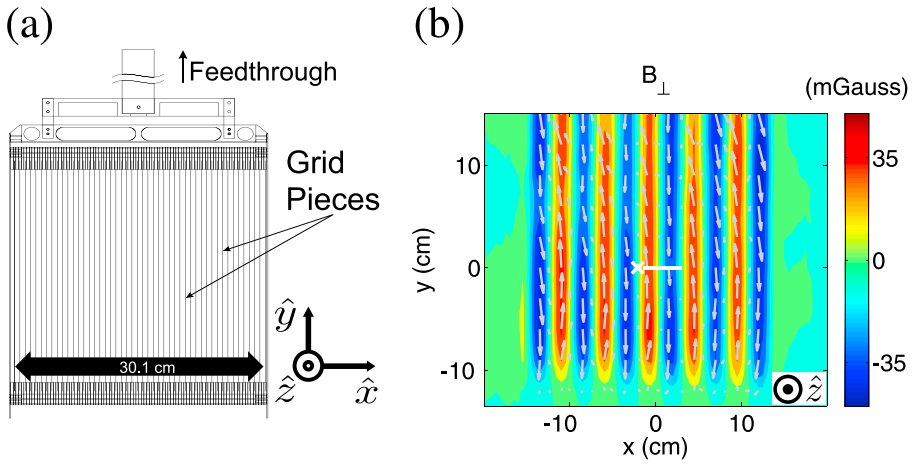

Figure 2. Alfvén waves are generated by the Arbitrary Spatial Waveform (ASW) antenna and observed using Elsässer probes. (a) The grid pieces of the ASW antenna can be phased independently to establish well-defined structure in $\hat{\mathbf{x}}$. (b) Elsässer probe measurements of $\mathbf{B}_\perp$ verify the planar Alfvén wave launched by the ASW antenna. Arrows show the amplitude and direction of $\mathbf{B}_\perp$; color is used to indicate the intensity of B_y. The white cross is the location of $g_e(v_z)$ measurements presented in Figures 3–4. Data from a scan along the white line are shown in Figure 5.

Elsässer probes [*Drake et al.*, 2011] resolve the magnetic and electric Alfvén wavefields in the *x-y* plane perpendicular to $\mathbf{B}_0$ using inductive coils and double probes. These probes are used to determine that the Alfvén wave amplitude is $B_y = 35$ mG so that $\delta B/B_0 \sim 2\times10^{-5}$, and $E_z = 110$ mV/m is calculated from Faraday's law using measurements of the perpendicular wavefields. A map of the measured transverse magnetic field in the plane perpendicular to $\mathbf{B}_0$ is shown in Figure 2b for a distance $z = 1.28$ m from the ASW antenna. For the inertial Alfvén wave generated in this experiment, $f = 125$ kHz and $k_z = 0.36 + 0.27i$ m^{-1}. Both damping and dispersion of the inertial Alfvén wave in the LaPD have been studied in previous work [*Thuecks et al.*, 2009; *Kletzing et al.*, 2010; *Nielson et al.*, 2010], finding that the damping of inertial Alfvén waves in the LaPD plasma is dominated by collisions in the moderately collisional core of the velocity distribution. The wave pattern in $\hat{\mathbf{x}}$ produced by the tuned ASW grid pieces gives $k_x\delta_e = 0.66$ with good spectral purity, $\delta k_x/k_x \sim 0.05$. The waveform travels with a group velocity effectively parallel to the fixed magnetic field $\mathbf{B_0}$.

Figure 1 also shows two *whistler probes* that are a part of the *Whistler Wave Absorption Diagnostic* (WWAD) [*Thuecks et al.*, 2012]. This diagnostic measures the suprathermal ($v_z > v_{te}$) portion of $g_e(v_z)$ and is based on a principle that was first implemented by *Kirkwood et al.* [1990]. A whistler mode wave is transmitted between the two whistler probes (1″ dipole antennas immersed in the plasma), and the attenuation of the received signal is used to determine the damping of the wave. Because the whistler wave is damped in proportion to the number of resonant electrons in the region between the antennas, the received amplitude is proportional to the resonant electron phase space density. The resonant electron velocity $v_z = 2\pi(|f_{ce}| - f_w)/k_z$ is specified by the electron cyclotron frequency $|f_{ce}| = 5.1$ GHz as well as the whistler wave's frequency f_w and parallel wave number k_z. Electrons at this velocity are Doppler shifted into resonance with the whistler wave. The diagnostic uses the attenuation of the whistler wave at frequency f_w to determine the part of the distribution function $g_e(v_z)$ that is Doppler shifted into resonance. The frequency f_w is chirped between $0.75 < f_w/|f_{ce}| < 0.95$ to obtain $g_e(v_z)$ for $3.5 < |v_z/v_{te}| < 9.5$. By alternating the direction of whistler propagation ($k_z > 0$ and $k_z < 0$), we measure $g_e(v_z)$ for $v_z > 0$ and $v_z < 0$.

Several aspects of the WWAD make it well suited for detecting how Alfvén waves modify $g_e(v_z)$ in the LaPD. First, in the frequency range used by the diagnostic, only the whistler wave propagates, and WWAD data can be unambiguously interpreted as whistler waves. This simplification results from the overdense plasma conditions of the LaPD, which are defined by $f_{pe}/|f_{ce}| > 1$. Second, because the whistler waves are at frequencies 10^4 times higher than the Alfvén modes, the whistler wave depends only on electron motion, making the diagnostic sufficiently responsive to the much slower variations of the electron population on the time scale of the Alfvén wave. Third, $g_e(v_z)$ measurements are localized to the 0.32 m region between the whistler probes. Since this length is much shorter than the 17.3 m Alfvén wavelength, the WWAD can detect variations in $g_e(v_z)$, as different phases of the Alfvén wave propagate past the point of measurement.

The experimental procedure is designed to measure the modifications of $g_e(v_z)$ due to the Alfvén wave launched by the ASW antenna. The most direct procedure would be to obtain several full scans of $g_e(v_z)$ within the period of the Alfvén wave, so that modifications on the time scale of the Alfvén wave could be resolved in real time. However, the f_w sweep rate, and therefore the time required to scan $g_e(v_z)$, is constrained by the electronics and sampling; the WWAD mixer's output frequency must be less than the LaPD digitizer's Nyquist frequency [see *Thuecks et al.*, 2012]. The consequence is that a full scan of $g_e(v_z)$ takes 10 μs, while the Alfvén wave period is 8 μs. Clearly, this direct procedure is not possible.

To relieve this constraint, an alternate approach is used that resolves Alfvén wave phase. Separate scans of $g_e(v_z)$ at different values of Alfvén wave phase are used to resolve the Alfvén wave period. At a given moment during the discharge sequence, the WWAD measures $g_e(v_z)$ at a particular velocity v_z, and at the same moment, the Alfvén wave will be at a phase ϕ_1. In a subsequent discharge the Alfvén wave phase is adjusted using the ASW antenna trigger. At the same moment in the discharge sequence, the WWAD measures $g_e(v_z)$ for the same velocity v_z, but the Alfvén wave is at a different phase ϕ_2. Measurements from these two separate discharges give $g_e(v_z)$ at v_z for ϕ_1 and ϕ_2. By extending this approach to 64 phase-shifted data sets, each set consisting of 1024 discharges to reduce random noise, a composite measurement is produced that records $g_e(v_z)$ as Alfvén wave phase evolves between 0 and 2π.

3. Theory

Before presenting $g_e(v_z)$ modifications detected using the experimental procedure, we will first discuss some of the theoretically expected properties of these modifications. Unlike the Alfvén waves of ideal MHD,

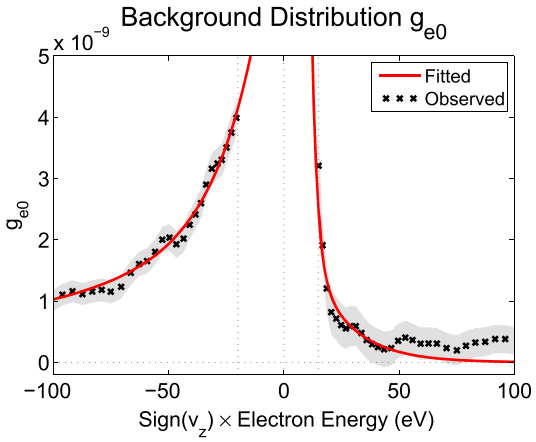

Figure 3. The measured background distribution function g_{e0}. Systematic errors, shown shaded, are due to whistler ducting. Dashed lines near +15 eV and −20 eV are the low-energy limit of WWAD measurements.

where the assumption $k_\perp \delta_e \ll 1$ results in no parallel electron motion, inertial Alfvén waves have $k_\perp \delta_e \sim 1$ which leads to a nonzero parallel electric field E_z, thereby enabling inertial Alfvén waves to modify the parallel electron motion [*Stasiewicz et al.*, 2000]. A calculation from *Kletzing* [1994] shows two effects of inertial Alfvén waves on parallel electron motion: the *sloshing* of the entire distribution $g_e(v_z)$ at the frequency of the Alfvén wave and the acceleration of electrons at the resonant velocity. The sloshing of $g_e(v_z)$ represents the oscillation of the density and current associated with the Alfvén wave itself. The resonant acceleration process is thought to underlie a significant fraction of auroral electron acceleration. Resonant acceleration occurs at the Alfvén wave phase speed, which in the case of inertial Alfvén waves is above the thermal speed since $v_A > v_{te}$. Because both sloshing and resonant acceleration are predicted to affect electrons with $v_z > v_{te}$, the WWAD was designed to measure $g_e(v_z > v_{te})$. *Kletzing* [1994] showed that both effects are a result of nonzero E_z and are expected to occur whenever inertial Alfvén waves propagate in the auroral magnetosphere. Until this study, neither effect has been directly measured.

Although fluid theories can often be used to describe the bulk activity of a plasma, a description of the suprathermal electron distribution requires kinetic theory. The Maxwell-Boltzmann system of equations is a starting point that not only accounts for the Alfvén wave but also captures the entire response of the electron distribution. We have produced a model for the periodic sloshing of $g_e(v_z)$ at the frequency of the Alfvén wave by linearizing this system of equations. To develop an analytically tractable theory, a number of reasonable assumptions are used, including that the waves are launched in a plasma with uniform density, temperature, and background magnetic field profiles. Additionally, the measured Alfvén wave pattern represented in Figure 2b is idealized as a linearly polarized waveform of infinite extent in the y direction. In order to describe parallel electron motion, the Boltzmann equation is integrated over transverse velocity to produce a dynamical equation for $g_e(v_z)$. The simplified Maxwell-Boltzmann system of equations is linearized, via the usual approach, to produce an inhomogeneous differential equation for the periodic electron sloshing $g_{e1}(v_z)$,

$$\frac{\partial g_{e1}}{\partial t} + v_z \frac{\partial g_{e1}}{\partial z} - \frac{e}{m_e} E_z \frac{\partial g_{e0}}{\partial v_z} = \left(\frac{\partial g_e}{\partial t} \right)_{\text{coll}} \tag{2}$$

In this equation $g_{e0}(v_z)$ is the static background distribution, m_e is the electron mass, e is the elementary charge, and E_z is the parallel electric field of the inertial Alfvén wave. The right-hand side models collisions with a Krook operator tested by *Thuecks et al.* [2009] using inertial Alfvén waves in the LaPD.

The periodicity of the Alfvén wave and the sloshing electron response allows a Fourier transform solution in time for $g_{e1}(v_z)$. A usable model for our experiment must account for the experiment's finite size along the z direction, which means that the relevant $g_{e1}(v_z)$ solution differs from the standard infinite space solution. In particular, the limited size of the experiment means a Fourier transform in space is not helpful. Instead, solutions are integrated in $\hat{\mathbf{z}}$ to account for the finite interaction length between the Alfvén wave and electrons. Additionally, a term is included to represent free-streaming electrons propagating into the bulk volume of the plasma from the boundary; these electrons are assumed to be a secondary effect of the voltage applied by the ASW antenna. This term takes the form of a homogeneous solution to equation (2).

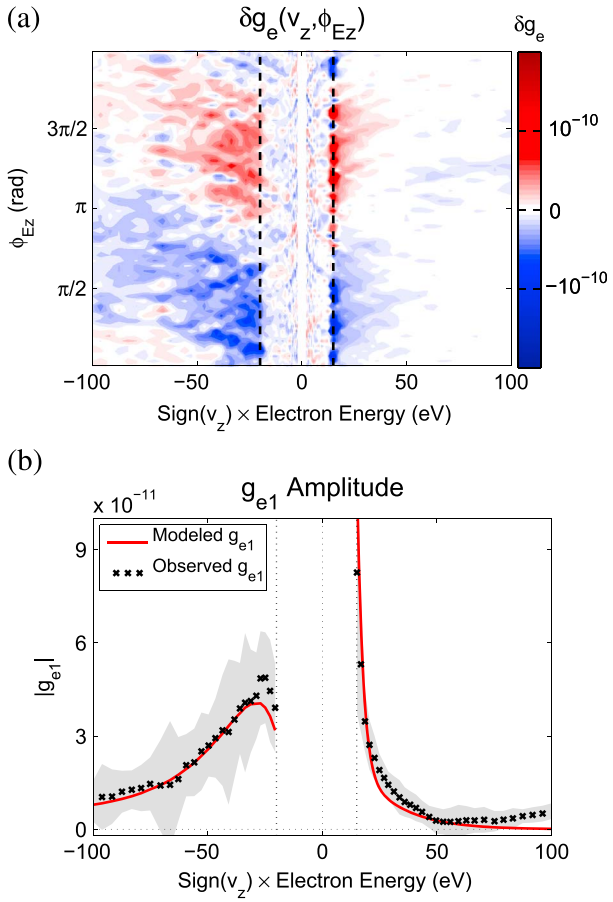

Figure 4. The composite measurement of $g_e(v_z)$ is generated using 64 phase-shifted data sets. (a) Sorting measurements by Alfvén wave phase and electron energy show that there are modifications of the electron distribution $\delta g_e = g_e - g_{e0}$ at the frequency of the Alfvén wave. (b) Magnitude of the first Fourier mode with respect to Alfvén wave phase compared to the solution of equation (2).

While the two effects predicted by *Kletzing* [1994] are qualitatively different, they are theoretically related. The linear solution $g_{e1}(v_z)$ for electron sloshing discussed here is needed for the nonlinear solution to the Maxwell-Boltzmann system of equations that captures resonant electron acceleration. Therefore, a test of electron sloshing $g_{e1}(v_z)$ is not only an important verification of basic inertial Alfvén wave behavior but also enables a future test of resonant electron acceleration.

4. Results

To compare the data with theory, we must extract $g_{e0}(v_z)$ and $g_{e1}(v_z)$ from the measurements. Because $g_e = g_{e0} + g_{e1} + \ldots$ and the modifications $g_{e1} + \ldots$ produced by the Alfvén wave are time periodic, these modifications can be removed from WWAD data by averaging over Alfvén wave phase to produce the experimental g_{e0}. The measured g_{e0} produced by this procedure is shown in Figure 3. The horizontal axis gives the resonant electron energy, $E = m_e v_z^2/2$, of each data point, and the sign of v_z has been maintained so that each half of the distribution function can be distinguished. Because the plasma is created by a hot-cathode discharge, it is expected that there are more suprathermal electrons moving away from the cathode with velocities $v_z < 0$, as is clearly seen in Figure 3. Smooth functions are fitted to each half of the experimental g_{e0} separately, and the derivatives $\partial g_{e0}/\partial v_z$ are used in equation (2) to produce the analytical solution for g_{e1}.

The random error in the measurement of g_{e0} is negligible. The dominant source of error is systematic and due to whistler ducting induced by the ~1% plasma density perturbation caused by inserting the whistler antennas into the plasma. This effect, which is well known, produces the low-amplitude undulations along the energy axis of the measured g_{e0} in Figure 3 [*Streltsov et al.*, 2012].

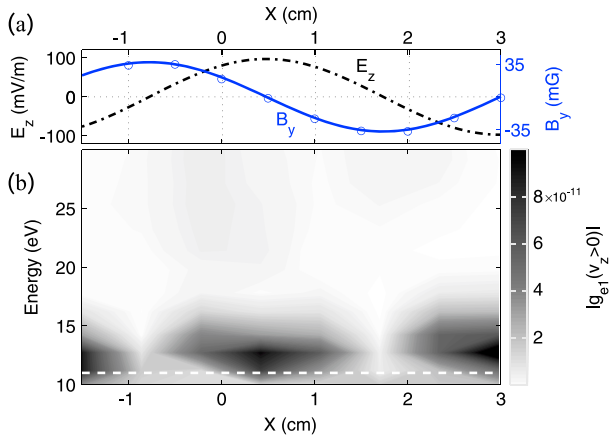

Figure 5. A cross-field scan shows the spatial correlation of the Alfvén wavefields and the measured intensity of g_{e1}. (a) Elsässer probe measurements of B_y along the range of the cross-field scan. E_z is inferred from Faraday's law. (b) The magnitude of g_{e1} from WWAD measurements for the same range in $\hat{\mathbf{x}}$. The extrema of g_{e1} and E_z are spatially coincident.

Figure 4a is the key experimental result of this letter. The background distribution has been removed so that the plotted quantity is $\delta g_e = g_e - g_{e0} \approx g_{e1}$. This plot shows the perturbation to the background electron distribution g_{e0} organized by Alfvén wave phase and electron energy. While this combination of axes may be unfamiliar, consider horizontal and vertical cuts separately. A horizontal cut shows how δg_e varies with electron energy at a fixed phase of the Alfvén wave. A vertical cut reveals the evolution of the perturbation to the parallel velocity distribution $g_e(v_z)$ at a fixed value of v_z as the Alfvén wave progresses through a phase of 2π; moving along the vertical axis shows how $g_e(v_z)$ evolves in phase through one Alfvén wave period. The primary feature of this plot is the periodic structure along the vertical axis. The period of δg_e matches that of the Alfvén wave, and we can conclude that $g_e(v_z)$ is being modified periodically at the frequency of the Alfvén wave. In other words, this plot shows electrons sloshing in the parallel electric field of the wave E_z, which is one of the most essential distinctions between MHD and inertial Alfvén waves.

The fundamental mode over phase seen Figure 4a is the linear response g_{e1}. Higher harmonics, if observed, can be attributed to nonlinear interactions. In this experiment, there are no nonlinear components detected above the noise level. Figure 4b shows the amplitude of the measured linear response g_{e1} extracted from Figure 4a using a Fourier transform over Alfvén wave phase. The amplitude of the measured g_{e1} agrees with the analytical solution of equation (2). The free-steaming term included in g_{e1} accounts for ~50% of the total solution.

The $g_e(v_z)$ measurements presented up to this point were taken at a single location, represented in the perpendicular plane by the white cross in Figure 2b. The white line in this same figure gives the range of a separate spatial scan across the $\mathbf{E}_\perp$ variation of the Alfvén wave that was also performed. The objective of this scan was to compare the spatial variations along the x direction of the Alfvén wavefields and the perturbed parallel distribution function $g_{e1}(v_z)$. Theory predicts that the parallel electric field E_z and the parallel electron currents are spatially coincident in the $\mathbf{E}_\perp$ direction due to their connection through the conductivity tensor. Since g_{e1} contains the parallel electron currents, we can predict that the extrema of E_z and g_{e1} should be spatially coincident. Figure 5a shows in more detail the Alfvén wavefields along this scan. The blue circles show Elsässer probe measurements of B_y. Errors associated with these measurements are smaller than the markers. E_z is calculated from B_y using Faraday's law. Figure 5b shows variations of the g_{e1} intensity along the scan. A comparison of Figures 5a and 5b shows that the extrema of g_{e1} and E_z align along the x direction, as predicted.

5. Conclusion

Our measurements have isolated the signatures of periodic electron motion, or *electron sloshing*, coherent with an inertial Alfvén wave, yielding resuts that are well described by linear theory. Although this physical behavior is not the resonant electron acceleration process believed to contribute to auroral generation, the electron sloshing detected here is predicted by the same theory. These measurements show modifications of the parallel electron motion at the Alfvén wave frequency, one of the most basic distinctions between MHD and inertial Alfvén waves. The measured perturbations of the reduced parallel electron distribution function,

designated as g_{e1}, have an amplitude and spatial structure consistent with the Alfvén wavefields. Despite a long history of invoking electron inertactions with inertial Alfvén waves to describe the auroral magnetosphere, this is the first direct observation of these interactions as manifested in the electron distribution function. To observe the nonlinear resonant acceleration process in the laboratory, using the same experimental wave-absorption technique will require the excitation of larger-amplitude Alfvén waves, the focus of the next phase of this project.

Acknowledgments
Supported by the NSF Graduate Research Fellowship under grant 1048957, NSF grants ATM 03-17310 and PHY-10033446, NSF CAREER award AGS-1054061, DOE grant DE-FG02-06ER54890, and NASA grant NNX10AC91G. The experiment presented here was conducted at the Basic Plasma Science Facility, funded by the U.S. Department of Energy and the National Science Foundation. The data used are available from the corresponding author upon request.

References

Bell, A. R. (1978), The acceleration of cosmic rays in shock fronts. I, *Mon. Not. R.. Astron. Soc.*, *182*, 147–156.
Chaston, C. C., C. W. Carlson, J. P. McFadden, R. E. Ergun, and R. J. Strangeway (2007), How important are dispersive Alfvén waves for auroral particle acceleration?, *Geophys. Res. Lett.*, *34*, L07101, doi:10.1029/2006GL029144.
Drake, D. J., C. A. Kletzing, F. Skiff, G. G. Howes, and S. Vincena (2011), Design and use of an Elsässer probe for analysis of Alfvén wave fields according to wave direction, *Rev. Sci. Instrum.*, *82*(10), 103505, doi:10.1063/1.3649950.
Gekelman, W., et al. (2016), The upgraded Large Plasma Device, a machine for studying frontier basic plasma physics, *Rev. Sci. Instrum.*, *87*(2), 25105, doi:10.1063/1.4941079.
Goertz, C. K., and R. W. Boswell (1979), Magnetosphere-ionosphere coupling, *J. Geophys. Res.*, *84*, 7239–7246, doi:10.1029/JA084iA12p07239.
Hasegawa, A. (1976), Particle acceleration by MHD surface wave and formation of aurora, *J. Geophys. Res.*, *81*, 5083–5090, doi:10.1029/JA081i028p05083.
Hollweg, J. V. (1974), Alfvénic acceleration of solar wind helium and related phenomena 1. Theory, *J. Geophys. Res.*, *79*, 1357, doi:10.1029/JA079i010p01357.
Keiling, A. (2009), Alfvén waves and their roles in the dynamics of the Earth's magnetotail: A review, *Space Sci. Rev.*, *142*, 73–156, doi:10.1007/s11214-008-9463-8.
Kirkwood, R., I. Hutchinson, S. Luckhardt, and J. Squire (1990), Measurement of suprathermal electrons in tokamaks via electron cyclotron transmission, *Nucl. Fusion*, *30*(3), 431.
Kletzing, C. A. (1994), Electron acceleration by kinetic Alfvén waves, *J. Geophys. Res.*, *99*, 11,095–11,104, doi:10.1029/94JA00345.
Kletzing, C. A., and S. Hu (2001), Alfvén wave generated electron time dispersion, *Geophys. Res. Lett.*, *28*, 693–696, doi:10.1029/2000GL012179.
Kletzing, C. A., D. J. Thuecks, F. Skiff, S. R. Bounds, and S. Vincena (2010), Measurements of inertial limit Alfvén wave dispersion for finite perpendicular wave number, *Phys. Rev. Lett.*, *104*(9), 95001, doi:10.1103/PhysRevLett.104.095001.
Lysak, R. L. (1985), Auroral electrodynamics with current and voltage generators, *J. Geophys. Res.*, *90*, 4178–4190, doi:10.1029/JA090iA05p04178.
McIntosh, S. W., B. de Pontieu, M. Carlsson, V. Hansteen, P. Boerner, and M. Goossens (2011), Alfvénic waves with sufficient energy to power the quiet solar corona and fast solar wind, *Nature*, *475*, 477–480, doi:10.1038/nature10235.
Nielson, K. D., G. G. Howes, T. Tatsuno, R. Numata, and W. Dorland (2010), Numerical modeling of Large Plasma Device Alfvén wave experiments using AstroGK, *Phys. Plasmas*, *17*(2), 22105, doi:10.1063/1.3309486.
Skilling, J. (1975), Cosmic ray streaming. I—Effect of Alfven waves on particles, *Mon. Not. R. Astron. Soc.*, *172*, 557–566.
Stasiewicz, K., et al. (2000), Small scale Alfvénic structure in the aurora, *Space Sci. Rev.*, *92*, 423–533.
Streltsov, A. V., J. Woodroffe, W. Gekelman, and P. Pribyl (2012), Modeling the propagation of whistler-mode waves in the presence of field-aligned density irregularities, *Phys. Plasmas*, *19*(5), 52104, doi:10.1063/1.4719710.
Thuecks, D. J., C. A. Kletzing, F. Skiff, S. R. Bounds, and S. Vincena (2009), Tests of collision operators using laboratory measurements of shear Alfvén wave dispersion and damping, *Phys. Plasmas*, *16*(5), 52110, doi:10.1063/1.3140037.
Thuecks, D. J., F. Skiff, and C. A. Kletzing (2012), Measurements of parallel electron velocity distributions using whistler wave absorption, *Rev. Sci. Instrum.*, *83*(8), 83503, doi:10.1063/1.4742766.